J Stat Phys (2008) 133: 617–637
DOI 10.1007/s10955-008-9618-8

On the Fluctuation Relation for Nosé-Hoover Boundary Thermostated Systems

Carlos Mejía-Monasterio · Lamberto Rondoni

Received: 12 October 2007 / Accepted: 13 August 2008 / Published online: 10 September 2008

Abstract We discuss the transient and steady state fluctuation relation for a mechanical system in contact with two deterministic thermostats at different temperatures. The system is a modified Lorentz gas in which the fixed scatterers exchange energy with the gas of particles, and the thermostats are modelled by two Nosé-Hoover thermostats applied at the boundaries of the system. The transient fluctuation relation, which holds only for a precise choice of the initial ensemble, is verified at all times, as expected. Times longer than the mesoscopic scale, needed for local equilibrium to be settled, are required if a different initial ensemble is considered. This shows how the transient fluctuation relation asymptotically leads to the steady state relation when, as explicitly checked in our systems, the condition found in (D.J. Searles, et al., J. Stat. Phys. 128:1337, 2007), for the validity of the steady state fluctuation relation, is verified. For the steady state fluctuations of the phase space contraction rate Λ and of the dissipation function Ω, a similar relaxation regime at shorter averaging times is found. The quantity Ω satisfies with good accuracy the fluctuation relation for times larger than the mesoscopic time scale; the quantity Λ appears to begin a monotonic convergence after such times. This is consistent with the fact that Ω and Λ differ by a total time derivative, and that the tails of the probability distribution function of Λ are Gaussian.

Keywords Nonequilibrium statistical mechanics · Fluctuation theorem · Thermostated systems · Heat condition

1 Introduction

In the last decades it has been recognized the central role that the fluctuations around stationary states play for a microscopic theory of nonequilibrium phenomena [1]. Furthermore, biological sciences and nano-technology are ever more interested in nonequilibrium fluctuations.

C. Mejía-Monasterio (✉) · L. Rondoni
Dipartimento de Matematica, Politecnico di Torino, corso Duca degli Abruzzi 24, 10129 Torino, Italy
e-mail: mejia@calvino.polito.it

The 1993 paper by Evans, Cohen and Morriss [2], on the fluctuations of the entropy production rate of a deterministic particle system, modeling a shearing fluid, provided a unifying framework for a variety of nonequilibrium phenomena, under a mathematical expression nowadays called *Fluctuation Relation* (FR). They proposed and tested the following formula

$$\frac{P(\overline{A}_\tau \in A_\delta)}{P(\overline{A}_\tau \in -A_\delta)} \simeq e^{\tau A}, \tag{1.1}$$

where $\overline{A}_\tau$ is the average of the power dissipated on evolution segments of duration τ, and $P(\overline{A}_\tau \in \pm A_\delta)$ is the probability that $\overline{A}_\tau$ takes a value in an interval of length δ, centered at $\pm A$. In analogy with the periodic orbit expansions [3, 4], (1.1), was obtained from the "Lyapunov weights" in the long τ limit. Remarkably, (1.1), does not contain any adjustable parameter.

In 1994, Evans and Searles obtained the first transient FRs for the energy dissipation rate divided by $k_B T$, denoted by Ω [5–11], which we call transient Ω-FR, and which concern the statistics of an evolving ensemble of systems, instead of the steady state statistics. The only requirement for the transient Ω-FR's to hold is the reversibility of the microscopic dynamics. Because they describe the behaviour of Ω, these relations can be experimentally verified [12].

In 1995, Gallavotti and Cohen provided a mathematical justification of the Lyapunov weights of Ref. [2], introducing the Chaotic Hypothesis [13–15], which states that: "A reversible many-particle system in a stationary state can be regarded as a transitive Anosov system,[1] for the purpose of computing its macroscopic properties". The result was a genuine steady state FR, which we call Λ-FR , as it concerns the fluctuations of the phase space contraction rate Λ. This quantity equals the energy dissipation rate Ω in a subclass of Gaussian isoenergetic particle systems, which includes the model of [2], while in many other cases Λ differs from Ω by a total derivative. As far as we know, the works [13–15] provide the only answer that has been given so far to the question of which dynamical systems can be proven to verify the steady state Λ-FR. A strong assumption as the Chaotic Hypothesis raises the question of which systems of physical interest are "Anosov-like", since almost none of them is actually Anosov. The answer of Refs. [13, 14] is that the Anosov property, in analogy with the Ergodic property, holds "in practice" for sufficiently chaotic, reversible systems.

A complementary approach, which addresses a different question, has been recently proposed in [16], developing ideas first introduced by Evans and Searles, see e.g. [5]. The question concerns the physical mechanisms at work in systems which do obey the steady state Ω-FR. This approach leads to a general framework within which various transient and steady state relations can be obtained for a variety of observables, and especially leads to the identification of physical mechanisms and time scales underlying the validity of the steady state FRs. The result is that, while the transient relations only rest on time reversibility, the steady state relations do require further properties to hold.[2] In [16], a property called "Ω-autocorrelation decay" is identified as the reason for the steady state Ω-FR, as well as of a number of other asymptotic relations, to be verified, when they do. This approach leads to the identification of the time scales concerning the FRs with the decay times of a quantity which we introduce in Sect. 3.3. Therefore, the need arises to test on concrete systems the

[1] Anosov systems are smooth and uniformly hyperbolic.

[2] For instance, the systems under consideration must converge towards a steady state.

validity of this identification and to quantify the corresponding time scales.[3] These issues are closely related with the role played in the dynamics by the singularities of the total derivative which distinguishes Λ from Ω. This has been discussed in various papers, like [17, 19, 23–25]. The present paper is devoted to the investigation of such questions.

We study the heat transport and its transient and steady state fluctuations, in a mechanical dissipative system that is maintained out of equilibrium by an imposed temperature gradient. This local thermostating mechanism leaves unaltered the Newtonian dynamics in the bulk of the system, dissipating only at its boundaries. However, due to the interactions, dissipation may depend on the non thermostated degrees of freedom (*d.o.f.*) as well [22]. To impose a temperature gradient we use deterministic Nosé-Hoover thermostats, that add a time-dependent friction term to the Hamiltonian of the system in such a way that, if the system is ergodic, the energy distribution of the thermostated *d.o.f.* is Boltzmann distributed with well defined temperature. As a consequence of the use of Nosé-Hoover thermostats, the phase space contraction rate is unbounded, possibly leading to statistical properties of its large fluctuations which are not described by the standard FR (1.1). This scenario has been considered in various works, and depends on the form of the tails of the distribution of the observables of interest, see e.g. [17, 19, 23–25]. As far as particle systems are concerned, the corresponding modified FR appears to be consistent with the Nosé-Hoover thermostated Lorentz gas [26]. In our case, consistently with the cited literature, the unboundedness of Λ does not imply any modification of the standard FR. The distribution of the fluctuations of Λ, indeed, appear to have Gaussian tails. Therefore, the search for deterministic particle systems which verify a modified version of FR, apart from the case of [26], must continue.

The paper is organized as follows: after defining the many-body dissipative model that we will use, in Sect. 2 we discuss the equilibrium and nonequilibrium states that arise from the coupling with the local thermostats. In Sect. 3 we study the transient Ω-FR and the steady state fluctuation relations for the phase space contraction rate, and for the dissipation function. Our conclusions are presented in Sect. 4.

2 The Model

The model we consider consists of a gas of non-interacting point-like particles of mass m that move freely inside a channel made of L identical two-dimensional cells. Each cell consists of a rectangular region of height Δy and width Δx, containing two fixed freely rotating disks of radius R and moment of inertia Θ.

The position of the disks in each cell and their radius are chosen so that the geometry of the channel corresponds to a periodic Lorentz gas in a triangular lattice at critical horizon, defined as the smallest disk radius to disks separation ratio such that the length of the particle's trajectory between two collisions with the disks is bounded. The lattice of scatterers is shown in Fig. 1. Moreover, the particles and disks are allowed to exchange energy at collisions, according to "perfectly rough" collisions, that are reversible, conserve total energy and angular momentum. These collisions are defined by the following formulae, which relate the normal and tangential components of the particle's velocity $\mathbf{v}$ with respect to the disk's surface, and the disk's angular velocity ω before (unprimed quantities) and after (primed quantities) the collision [27]

$$v_n' = -v_n,$$

[3] A similar study of the time scales was performed in Ref. [18], in one investigation on the applicability of the Chaotic Hypothesis.

$$v_t' = v_t - \frac{2\eta}{1+\eta}(v_t - R\omega), \tag{2.1}$$

$$R\omega' = R\omega + \frac{2}{1+\eta}(v_t - R\omega).$$

Thus, collisions are deterministic, time-reversible and phase space volume preserving. The parameter η, defined as

$$\eta = \frac{\Theta}{mR^2}, \tag{2.2}$$

is the only relevant dimensionless parameter characterizing the collision. It determines the energy transfer between disks and particles in a collision. For finite values of η, the particles indirectly exchange energy with each other, through the interactions with the disks, even though they do not directly interact.

This model, introduced in [27] as a mechanical model for coupled heat and matter transport, shows realistic equilibrium and out of equilibrium thermodynamical properties, in very different situations, e.g. when subjected to external gradients of temperature and chemical potential, in the presence of external electric or magnetic fields [28].

The simple energy exchange mechanism allows the equipartition of the energy among all the *d.o.f.*, allowing the system to reach a local thermal equilibrium. In particular, in microcanonical simulations, the particle velocities are Maxwellian distributed at uniform "temperature" consistent with the equipartition theorem. These temperatures also characterize the distribution of angular velocities of the rotating scatterers. The same is true in canonical and grancanonical simulations, where the system is subjected to temperature and chemical potential gradients. One consequence of the establishment of local thermal equilibrium is that the gas of particles is described locally by the equations of state of ideal gases. Recently, the properties of the stationary state for a modified version of this model, coupled to stochastic energy and particles reservoirs, have been analytically obtained in the weak coupling limit [29], and finite coupling corrections have been obtained in [30].

2.1 Local Nosé-Hoover Thermostats

To establish a nonequilibrium state, two heat baths are placed at the left and right boundaries of the model, with local temperatures set to T_C and T_H respectively. In previous works [27–30], the bulk of the system was coupled to stochastic thermochemical baths, so to exchange energy and particles at the boundaries. Differently, we consider a closed system (particle number is conserved), and model the heat baths as local Nosé-Hoover thermostats [31]. Roughly speaking a Nosé-Hoover thermostat adds a kind of friction term to a number of degrees of freedom, whose energy fluctuations turn to be canonical at some temperature T, as a result.

More precisely, consider n_{th} *d.o.f.* with generalized positions q, momenta π and mass m, subjected to an external potential $\phi(\vec{q})$ described by the Nosé Hamiltonian [32],

$$H_{n_{\text{th}}}(\vec{q}, \vec{\pi}, X, \Xi, s) = \sum_{i=1}^{n_{\text{th}}} \frac{\pi_i^2}{2mX^2} + \phi(\vec{q}) + \frac{\Xi^2}{2Q} + (g+1)k_B T \ln X. \tag{2.3}$$

Here X and Ξ are the generalized position and momentum of the thermostat and Q its effective mass. s is a generalized time variable, T the temperature, g a number related to n_{th} and k_B the Boltzmann constant. If one identifies s and π with the physical time t and

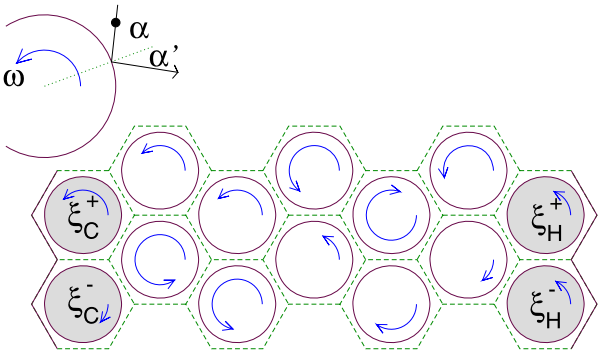

Fig. 1 Geometry of a system of length $L = 7$ cells. The disks of radius R form a triangular lattice at critical horizon, meaning that the height and width of the cells equal, respectively, $\Delta x = 2R$ and $\Delta y = 2W$, where $W = 4R/\sqrt{3}$ is the separation between the centers of the disks. Periodic boundary conditions along the vertical direction are considered. The *dashed lines* indicate the single hexagonal cells. The *solid lines* are hard walls. At the *left top* we schematically show a single collision: when a particle collides with a disk at an angle α with respect to the normal at the collision point, the outgoing angle of its trajectory α' is determined by (2.1). In between collisions, the angular velocity of the disk ω evolves freely for the disks in the bulk (*empty disks*) and according to (2.5) for the thermostated disks (*filled disks*)

momenta p, letting $\mathrm{d}s = X\mathrm{d}t$ and $\pi_i = Xp_i$, and additionally $g = n_{\mathrm{th}}$ then, it is easy to show that if the generalized variables $\vec{\pi}$, X and Ξ are distributed microcanonically, then the physical variables $\vec{q}$ and $\vec{p}$ are distributed according to the canonical distribution with temperature T [33].

Furthermore, if one is solely interested in real time averages, the equations of motion that derive from (2.3) can be rewritten in terms of the physical variables $\vec{q}$, $\vec{p}$ and t, eliminating the variables X, Ξ, $\vec{\pi}$ and s to obtain [31],

$$\begin{aligned} \dot{q}_i &= \frac{p_i}{m}, \\ \dot{p}_i &= -\nabla\phi - \xi p_i, \\ \dot{\xi} &= \frac{1}{\tau_{\mathrm{th}}^2}\left(\frac{1}{n_{\mathrm{th}}k_{\mathrm{B}}T}\sum_{i=1}^{n_{\mathrm{th}}}\frac{p_i^2}{m} - 1\right), \end{aligned} \tag{2.4}$$

where τ_{th} is the relaxation time of the thermostat related to its effective mass Q as $\tau_{\mathrm{th}}^2 = Q/n_{\mathrm{th}}k_{\mathrm{B}}T$ and $\xi = \Xi/Q$, (in what follows we will refer to the variable ξ as the thermostat). Inspecting (2.4), known as the Nosé-Hoover equations of motion, the role of the thermostat ξ becomes evident: it acts as a friction term that appropriately changes sign, depending on whether the instantaneous kinetic energy of the n_{th} thermostated *d.o.f.* is larger or smaller than the desired mean kinetic energy $n_{\mathrm{th}}k_{\mathrm{B}}T/2$.

To simulate a nonequilibrium state, we couple Nosé-Hoover thermostats to the angular velocity of each of the four disks at the boundaries of the channel. Since the disks are pinned to their positions, the thermostats can interact with the rest of the *d.o.f.* only via the collisions with the point-like moving gas particles. We denote by ξ_{C}^{+} and ξ_{C}^{-} the thermostats for the upper and lower disks at the cold side and as ξ_{H}^{+} and ξ_{H}^{-} the thermostats for the upper and lower disks at the hot side, thus $n_{\mathrm{th}} = 1$. Note that it is possible to couple the two disks at each boundary to one single thermostat, in which case, $n_{\mathrm{th}} = 2$. We have chosen the former

coupling as we get more efficient numerics than in the latter case. Also, we assume that there is no external potential ϕ acting on the particles.

In [34], it has been shown that the Nosé-Hoover dynamics are not ergodic for $\phi = 0$, thus the phase space probability distribution is not canonical. However, as we will see, the interaction of the thermostated disks with the gas of particles leads to ergodic motions in the accessible phase space.

Labeling the cells of the channel from 1 to L, the equations of motion for our model can be written as follows

$$\begin{aligned}
\dot{q}_i &= \frac{p_i}{m}; \quad i = 1, \ldots, n \\
\dot{p}_i &= \Upsilon_{\eta;i}(t); \quad i = 1, \ldots, n \\
\dot{\omega}_j^{\pm} &= \Upsilon_{\eta;j}^{\pm}(t); \quad j = 2, \ldots, L-1 \\
\dot{\omega}_{\mathrm{C}}^{\pm} &= \Upsilon_{\eta;\mathrm{C}}^{\pm}(t) - \xi_{\mathrm{C}}^{\pm}\omega_{\mathrm{C}}^{\pm}, \\
\dot{\omega}_{\mathrm{H}}^{\pm} &= \Upsilon_{\eta;\mathrm{H}}^{\pm}(t) - \xi_{\mathrm{H}}^{\pm}\omega_{\mathrm{H}}^{\pm}, \\
\dot{\xi}_{\mathrm{C}}^{\pm} &= \frac{1}{\tau_{\mathrm{th}}^2}\left(\frac{\Theta\omega_{\mathrm{C}}^{\pm 2}}{k_{\mathrm{B}}T_{\mathrm{C}}} - 1\right), \\
\dot{\xi}_{\mathrm{H}}^{\pm} &= \frac{1}{\tau_{\mathrm{th}}^2}\left(\frac{\Theta\omega_{\mathrm{H}}^{\pm 2}}{k_{\mathrm{B}}T_{\mathrm{H}}} - 1\right),
\end{aligned} \tag{2.5}$$

where n is the number of particles. The abstract operators $\Upsilon_\eta(t)$, represent the instantaneous forces exerted on particles and disks during a collision. They are subjected to the condition

$$\sum_{i=1}^{n} \frac{p_i}{m}\Upsilon_{\eta;i}(t) + \sum_{\substack{i=2 \\ \{+,-\}}}^{L-1} \Theta\omega_i \Upsilon_{\eta;i}(t) + \sum_{\{+,-\}} \Theta\left(\omega_{\mathrm{C}}\Upsilon_{\eta;\mathrm{C}}(t) + \omega_{\mathrm{H}}\Upsilon_{\eta;\mathrm{H}}(t)\right) = 0, \tag{2.6}$$

which accounts for the conservation of energy during the collisions.

The dynamics (2.5) is dissipative as the phase space volume contracts at a rate given by

$$\Lambda \equiv -\mathrm{div}_\Gamma \dot{\Gamma} = \xi_{\mathrm{C}}^{-} + \xi_{\mathrm{C}}^{+} + \xi_{\mathrm{H}}^{-} + \xi_{\mathrm{H}}^{+}, \tag{2.7}$$

where $\Gamma \equiv (\vec{q}, \vec{p}, \vec{w}, \vec{\xi})$. The mean value of the phase space contraction rate Λ is zero only at equilibrium, i.e., when $T_{\mathrm{H}} = T_{\mathrm{C}}$. As we will see in Sect. 3.2, the cold thermostats contract the phase space volume at a rate faster than the expansion produced by the hot thermostats so that on average, Λ is positive.

2.2 Ergodicity and Equilibrium State

Because our system is not subjected to any external field, the thermostats dissipate energy only when they collide with the particles. These collisions, in turn, make apparently ergodic the evolution of the thermostated *d.o.f.*, since the particles dynamics is randomized by the motion in the bulk of the system. To illustrate this, we have considered the dynamics inside one single hexagonal cell (see Fig. 1), containing a thermostated disk and $n = 10$ particles, with reflecting boundary conditions. In Fig. 2, the evolution of the thermostat ξ and the angular velocity of the disk ω is shown for a temperature $T = 1000$. In the main panel,

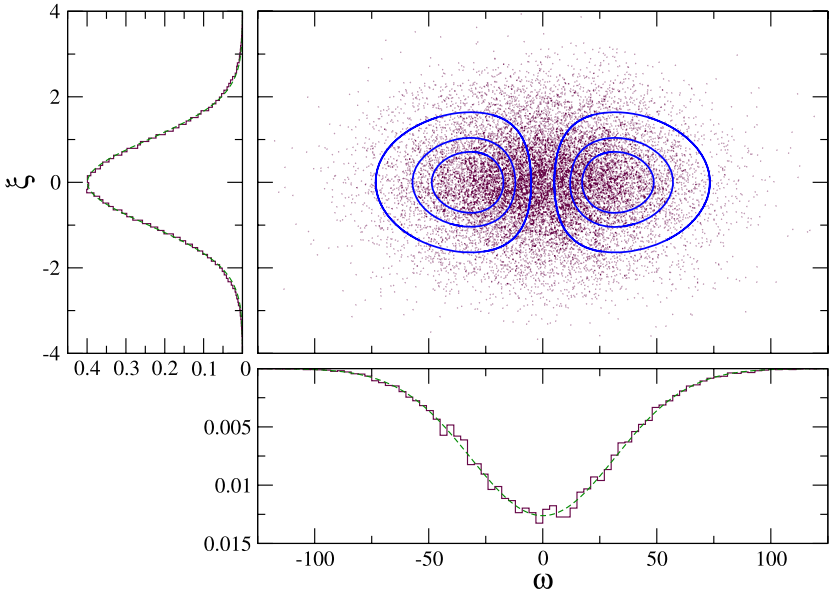

Fig. 2 *Main panel*: Evolution of the angular velocity of the disk $\omega(t)$ and its thermostat $\xi(t)$ for the one single cell at a temperature $T = 1000$, in the presence (*dots*) and absence (*solid curves*) of the gas of particles. In the presence of the particles the trajectory is obtained from one initial condition. The *solid curves* correspond to three pairs of symmetric initial conditions. *Secondary panels*: histograms of the marginal distributions $P(\xi)$ (*left*) and $P(\omega)$ (*lower*) of the trajectory with interactions. The *dashed curves* are the corresponding equilibrium distributions

the solid curves correspond to the evolution of the isolated thermostated disk, i.e., without the interaction with the gas of particles, for three pairs of symmetric initial conditions. In this case, the evolution of the vector (ω, ξ) is oscillatory: ω oscillates around its equilibrium value $\sqrt{T}$, preserving its initial sign. The thermostat ξ oscillates symmetrically around zero. Differently, when particles are allowed to interact with the disk, the trajectory of any initial condition explores all the available phase space, as shown by the cloud of points in the main panel of Fig. 2. Furthermore, the histograms in the left and lower panels correspond to the marginal distributions of the points of the trajectory, which coincide with the corresponding equilibrium distributions of ξ and ω (dashed curves).

Summarizing, while in the absence of interactions the dynamics of the disk is trivial (periodic), the interactions with the particles lead to trajectories which appear to explore all the available (ω, ξ) space. This apparent ergodicity, combined with the observation that the distribution of the particles velocities approximates a Maxwellian at the temperature T, indicates that locally (in the cell) a form of thermal equilibrium is established.

In the single cell we also have computed the energy probability distribution function $P(E)$ of the disk and of the energy of the gas of particles, for a given temperature $T = 100$. The results are shown in Fig. 3. The agreement with the theoretical equilibrium Boltzmann distributions is excellent. Independently of the initial state, the gas of particles and the thermostated disk reach quite rapidly ($\mathcal{O}(10^4)$ collisions times) the equilibrium state at a temperature equal to that of the thermostat. For the model depicted in Fig. 1 a uniform equilibrium state is established if $T_C = T_H = T$.

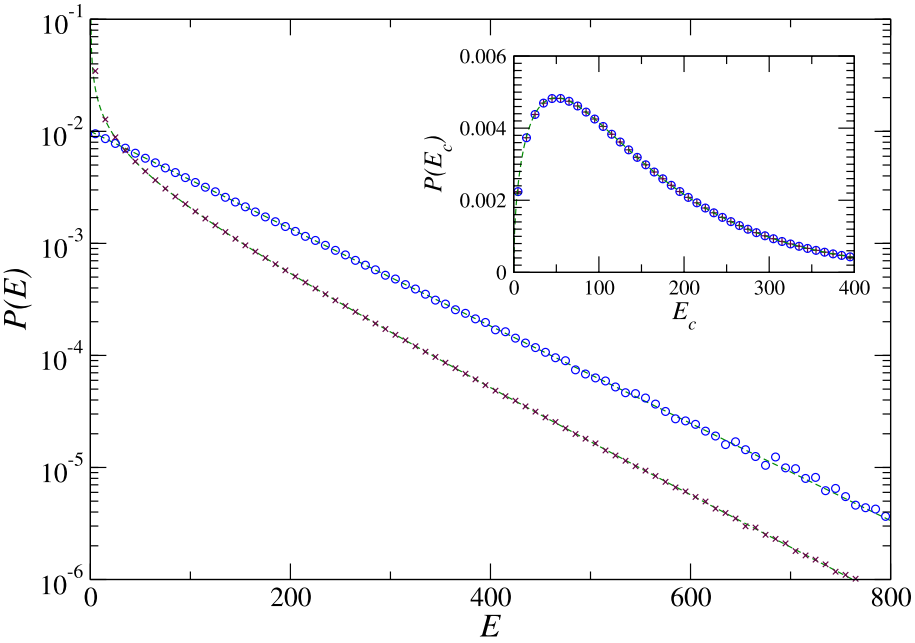

Fig. 3 Equilibrium energy probability distribution $P(E)$ for the disk (*crosses*) and particles (*circles*). The distributions were obtained for 10 particles in a hexagonal cell containing one single disk thermostated at a temperature $T = 100$. The dashed lines correspond to the theoretical equilibrium distributions. *Inset*: Conditional probability distribution of the energy of the particles $P(E_c)$, before (*circles*) and after (*plus*) the collisions. The dashed line corresponds to the theoretical distribution function

A similarly fast relaxation to equilibrium, due to the interaction of (2.1), was also observed using stochastic baths [27, 28]. The local equilibration between the thermostated and not thermostated *d.o.f.* is due to the fact that, at the collisions, the incoming and outgoing temperatures dynamically relax to the same value. In the inset of Fig. 3 the incoming and outgoing energy probability distribution function conditioned to the occurrence of a collision is shown. Both PDF coincide. Moreover, they coincide with the theoretical equilibrium conditional probability (shown as a solid line). This is a remarkable feature of the present model which is not always obtained in other systems [35].

Note that the same qualitative results are found independently of the particle's density n. However, the time required to reach equilibrium with the gas of particles is determined by the rate $\gamma \propto n\sqrt{T}$ at which the gas of particles collides with the thermostated disk, compared to the relaxation time τ_{th} of the thermostat.

Also note that the thermostated *d.o.f.* ω changes discontinuously at collision, while the thermostat variable ξ does not. We have not observed any noticeable consequence of the uncoupled evolution of ξ and ω at the collisions. We expect that this will affect the efficiency of the thermostat, at most. A similar observation was made in [34], for a thermostat with same kind of discontinuities.

2.3 Nonequilibrium Steady State

We now turn our attention to nonequilibrium states. In [27, 28] the transport properties of the system of Sect. 2 were studied. The system was coupled to stochastic thermochemical

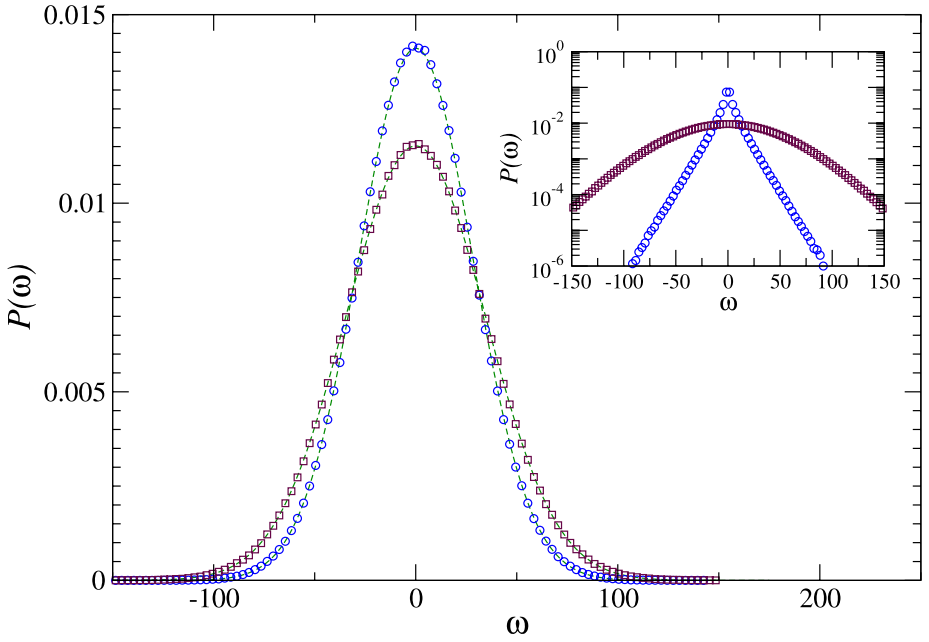

Fig. 4 Probability distribution function of the angular velocity $P(\omega)$ of the "cold" (*circles*) and hot (*squares*) thermostated disks, from a simulation with $T_C = 900$ and $T_H = 1100$, $n = 20$ particles per cell and $L = 7$ cells. The *dashed lines* correspond to the theoretical equilibrium distribution functions. In the *inset*, the same distributions are shown, for a much larger temperature gradient of $T_C = 100$ (circles) and $T_H = 1900$

baths to create temperature and chemical potential gradients. In that configuration, it was found that the hypothesis of local thermal equilibrium holds and that the deviations from it are consistent with the transport of heat and matter that appears as a response to the external gradients. LTE results from the mixing properties of the effective interaction among particles. In the absence of interaction, e.g., when $\eta = 0$, LTE is not satisfied (see e.g., [36]).

In our present situation, the stochastic baths are substituted by deterministic Nosé-Hoover thermostats. Moreover, the Lorentz channel is closed, i.e., there is no exchange of particles between the system and the reservoirs, implying that the particle current is zero.

Since LTE is a consequence of the mixing due to the interactions, we have observed that it holds, indeed, in the bulk.[4] However, away from equilibrium, this is not necessarily the case in the thermostated regions. In order to understand how effectively the interactions establish LTE in the neighbourhood of the thermostated disks, we have performed extensive numerical simulations, at different temperature gradients. In Fig. 4 we show the probability distribution function of the angular momentum of the thermostated disks $P(\omega)$, for a temperature gradient of $T_C = 900$ and $T_H = 1100$. The circles and the squares correspond to the distribution of the disks at the cold and hot sides, respectively. The dashed lines correspond to the theoretical equilibrium distributions at the nominal temperatures of the thermostats T_C and T_H. The agreement of $P(\omega)$ with their respective theoretical distributions is excellent.

However, for very large temperature gradients, LTE is not established at the cold side, while the LTE at the hot side does not necessarily correspond to the chosen T_H. For instance,

[4] By bulk we mean all cells which do not contain a thermostated disk (open disks in Fig. 1).

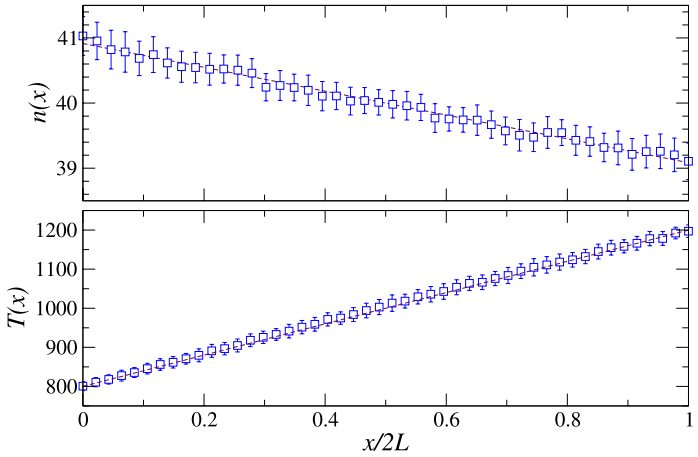

Fig. 5 Stationary profiles of the density $n(x)$ and the energy density $T(x)$ of the particles from a simulation with $T_C = 800$ and $T_H = 1200$, $n = 10$ particles per cell and $L = 48$ cells. The *dashed lines* correspond to a linear profile between T_C and T_H, (*lower panel*), and to a best linear fit of $n(x)$, (*upper panel*). Note, however, that for our system neither $T(x)$ nor $n(x)$ need to be linear

the inset of Fig. 4 shows the cold and hot $P(\omega)$ for $T_C = 100$ and $T_H = 1900$. The exponential tails of $P(\omega)$ at the cold side is a signature of the bad equilibration. While at the hot side $P(\omega)$ remains Gaussian, but its variance corresponds to a temperature which is not T_H. The bad equilibration around the cold side is due to the inefficiency of the thermostat to thermalize the much more energetic particles coming from the hot region. Thus, the bulk of the system practically equilibrates with the hot thermostat alone. This problem can be partially solved by varying the relaxation time of the cold thermostat τ_{th}. However, the state at the cold side is very sensitive to variations of τ_{th}, which must be determined case by case. In the following we restrict our computations to gradients $\Delta T/T \leq 1$, for which LTE, at the correct temperatures is established.

In all cases we have found that the steady state is characterized by linear particle $n(x)$ and energy $T(x)$ density profiles. In Fig. 5, we show an example of $n(x)$ and $T(x)$ for a chain of 48 cells and 10 particles per cell, with $T_C = 800$ and $T_H = 1200$. Note that the temperature gradient generates a particle density gradient, in the bulk. However, since the billiard model that we consider is closed, the mean particle current is zero. Note also that $T(x)$ does not jump at the boundaries, which means that a good equilibration between thermostats and gas particles is achieved. By measuring the heat current as a function of the size of the system, for a fixed temperature difference, we verified the validity of Fourier's law to high accuracy.

The same results had been previously obtained in [27, 28], for the system coupled to stochastic thermochemical baths. It is indeed expected that the transport properties in the bulk of the system do not depend on the particular model of heat bath.

3 Fluctuation Relation for Heat Conduction

In this section we study the fluctuations of the phase space contraction rate and of the entropy production, or energy dissipation in the transient response to external drivings and in the stationary state of the model system introduced in Sect. 2.

3.1 Transient Fluctuation Relation

Consider a system that is initially at equilibrium. At time $t = 0$, an external force, either mechanical or thermodynamical, is applied. For times $t > 0$ the system evolves from its equilibrium state towards, possibly, a nonequilibrium steady state. In the process, the system dissipates the work that the external forcing performs on it. Furthermore, consider an ensemble of trajectories in the phase space Γ, that originate at the equilibrium state (at $t = 0$) and evolve for a finite time τ. For $\delta > 0$, let $A_\delta^+ = (A-\delta, A+\delta)$ and $A_\delta^- = (-A-\delta, A+\delta)$. The Transient Fluctuation Relation [37], states that

$$\ln \frac{\text{Prob}(E(\overline{\Omega}_{0,\tau} \in A_\delta^+))}{\text{Prob}(E(\overline{\Omega}_{0,\tau} \in A_\delta^-))} \simeq A\tau, \tag{3.1}$$

where $E(\overline{\Omega}_{0,\tau} \in (a,b))$ is the set of points in Γ, such that $\overline{\Omega}_{0,\tau} \in (a,b)$[5] and $\overline{\Omega}_{0,\tau} = (1/\tau)\int_0^\tau \Omega(\Gamma(t))dt$ is the time averaged *dissipation function*, which is defined in terms of the (initial) phase space probability density f and of the phase space contraction rate Λ as [37]:

$$\overline{\Omega}_{0,\tau}(\Gamma) \equiv \frac{1}{\tau}\left(\ln \frac{f(\Gamma)}{f(\mathcal{S}^\tau\Gamma)} + \int_0^\tau \Lambda(\Gamma(t))dt\right). \tag{3.2}$$

Remark 3.1 The density f can be arbitrarily chosen. However, if it represents the equilibrium ensemble associated with the chosen dynamics, then Ω corresponds to the physical dissipation (the entropy production, close to equilibrium) [16].

In this section we study the fluctuations of the time averaged dissipation function as the system moves away from a given equilibrium state. In Ref. [38], a transient fluctuation formula for heat conduction was obtained, considering a generic system coupled to two (deterministic) thermostats, which is the case of the present work. In Ref. [16] the transient fluctuation relation has then been obtained in great generality for Ω, under the sole assumption of time reversibility. Hence we recall the definitions of [16], which will be used for the steady state fluctuation relations as well.

Consider a dynamical system with phase-space $\mathcal{M}$, described by an evolution operator $\mathcal{S}^t : \mathcal{M} \to \mathcal{M}$. Let $\mathcal{S}^t$ be reversible, i.e. such that for an involution $i : \mathcal{M} \to \mathcal{M}$ representing the time inversion operator, $i\mathcal{S}^t\Gamma = \mathcal{S}^{-t}i\Gamma$ holds for all $\Gamma \in \mathcal{M}$ and all $t \in \mathbb{R}$. Introduce a probability measure μ with density f on $\mathcal{M}$, i.e. $d\mu(\Gamma) = f(\Gamma)d\Gamma$, which is even for i, i.e. $f(i\Gamma) = f(\Gamma)$. Let $\phi : \mathcal{M} \to \mathbb{R}$ be any odd observable, i.e., $\phi(i\Gamma) = -\phi(\Gamma)$, of a many-body dynamical system that satisfies the assumptions above and denote by

$$\overline{\phi}_{0,\tau} = \frac{1}{\tau}\int_0^\tau \phi(\mathcal{S}^t\Gamma)dt,$$

the time average of ϕ during a time τ with initial condition Γ.

In [16] it was proved that ϕ satisfies the following symmetry relation:

$$\frac{\mu(\overline{\phi}_{0,\tau} \in A_\delta^+)}{\mu(\overline{\phi}_{0,\tau} \in A_\delta^-)} = \langle e^{-\Omega_{0,\tau}}\rangle^{-1}_{\overline{\phi}_{0,\tau} \in A_\delta^+}, \tag{3.3}$$

[5] In what follows, we will omit the specification of the set E for the sake of simplicity.

where $\Omega_{0,\tau}(\Gamma) = \tau\overline{\Omega}_{0,\tau}(\Gamma)$ is the time integral of Ω over the interval $[0, \tau]$. In the *r.h.s.* of (3.3) the average $\langle\cdot\rangle_{\overline{\phi}_{0,\tau}\in A^+_\delta}$ is the ensemble average over the set of trajectories that satisfy the constraint that $\overline{\phi}_{0,\tau} \in A^+_\delta$. The Conditional reversibility theorem derived in Ref. [39] is related to the steady state version of (3.3), given in [16].

When the system is subjected to an external mechanical force $\vec{F}$, the density function leading to the physical dissipation is the equilibrium ($\vec{F} = 0$) probability density. Other choices are possible and, for instance, the uniform density in a compact phase space, $f(\Gamma) = 1/|\mathcal{M}|$, yields $\Omega = \Lambda$, the phase space contraction rate.

Remark 3.2 The relation (3.3) is exact. It is purely a consequence of the time reversibility of the dynamics. Remarkably, this relation is valid for any observable that is odd with respect to time reversal.

In particular, we can take $\overline{\Omega}_{0,\tau}$ as the observable. Doing so, (3.3) becomes

$$\begin{aligned}\frac{\mu(\overline{\Omega}_{0,\tau} \in A^+_\delta)}{\mu(\overline{\Omega}_{0,\tau} \in A^-_\delta)} &= \langle e^{-\tau\overline{\Omega}_{0,\tau}}\rangle^{-1}_{\overline{\Omega}_{0,\tau}\in A^+_\delta} \\ &= e^{[A+\varepsilon(\delta,A,\tau)]\tau},\end{aligned} \tag{3.4}$$

where the error term $\varepsilon \leq \delta$, in general will depend on δ, A and τ. In [16] the transient fluctuation relation (3.4) was called Ω-FR.

3.2 Dissipation Function for Heat Flow

In this section we investigate the transient response of the system of Sect. 2 to a temperature gradient. The dynamics of the model is given by the equations of motion (2.5) and the energy density of the system H, can be written as

$$\begin{aligned}H(\vec{p},\vec{\omega},\vec{\xi}) = \frac{1}{2m}\sum_{i=1}^{n} p_i^2 + \frac{\Theta}{2}\sum_{j=1}^{L}\left[(\omega_j^+)^2 + (\omega_j^-)^2\right] \\ + \frac{\tau_{\text{th}}^2}{2}\sum_{\{+,-\}}\left(T_{\text{C}}\xi_{\text{C}}^2 + T_{\text{H}}\xi_{\text{H}}^2\right),\end{aligned} \tag{3.5}$$

where $\omega_1^\pm = \omega_{\text{C}}^\pm$ and $\omega_L^\pm = \omega_{\text{H}}^\pm$. Here, $\xi_{\text{C}} = \xi_{\text{C}}^- + \xi_{\text{C}}^+$ and $\xi_{\text{H}} = \xi_{\text{H}}^- + \xi_{\text{H}}^+$. We consider the following transient process:

At times $t < 0$ the system and the thermostats are in thermal equilibrium at some temperature T_0. For simplicity we choose the equilibrium temperature as $T_0 = (T_{\text{C}} + T_{\text{H}})/2$ (in the linear regime T_0 is the mean temperature of the steady state of the system). Therefore, the initial density distribution corresponds to the canonical equilibrium distribution

$$f(\Gamma) = \frac{e^{-\beta_0 H(\Gamma)}}{\int d\Gamma e^{-\beta_0 H(\Gamma)}}, \tag{3.6}$$

with $\beta_0 = 1/k_{\text{B}}T_0$, and $H(\Gamma)$ the energy density (3.5), with $T_{\text{C}} = T_{\text{H}} = T_0$. At time $t = 0$ the temperatures of the thermostats are set to T_{C} for the *cold* thermostat and T_{H} for the *hot* one. At times $t > 0$ the system is not in equilibrium and a heat flux develops.

We measure the transient response of the system by considering time averages during a finite time τ of the dissipation function Ω.

Substituting (3.6) into (3.2), the time average of $\overline{\Omega}_{0,\tau}$ takes the simple form

$$\overline{\Omega}_{0,\tau}(\Gamma) = \frac{1}{\tau}\int_0^\tau \left(\beta_0 \dot{H}(S^t\Gamma) + \Lambda(S^t\Gamma)\right) dt = \beta_0 \left(\frac{H(S^t\Gamma) - H(\Gamma)}{\tau}\right) + \overline{\Lambda}_{0,\tau}(\Gamma). \quad (3.7)$$

The quantities Ω and Λ, thus differ by a total time derivative, as in the cases considered in e.g. [17, 18, 25, 26]. Taking the time derivative of (3.5) and using the constraint (2.6) we obtain

$$\dot{H}(t) = -\left(T_C\xi_C + T_H\xi_H\right). \quad (3.8)$$

Finally, using the expression for the phase space contraction rate (2.7), the time averaged dissipation function for the heat flow of our model becomes

$$\overline{\Omega}_{0,\tau}(\Gamma) = \frac{T_H - T_C}{T_H + T_C}\left(\overline{\xi}_{C;\,0,\tau} - \overline{\xi}_{H;\,0,\tau}\right). \quad (3.9)$$

As a test of the physical character of the dissipation function (3.9), we have computed its long time average in the steady state, $\overline{\Omega}_{0,\tau}$, as a function of the relative temperature gradient $\Delta T/T$. This is shown in Fig. 6 for a chain of 5 cells and 20 particles per cell. For each simulation the temperatures of the thermostats T_C and T_H were varied symmetrically around $T = 1000$. At equilibrium $\overline{\Omega}_{0,\tau} = 0$. Out of equilibrium, $\overline{\Omega}_{0,\tau}$ grows with the external gradient as $(\Delta T/T)^2$. In the inset of Fig. 6 we show the average behaviour of the individual thermostats $\overline{\xi}_C$ and $\overline{\xi}_H$. At equilibrium, both thermostats average to zero. Away from equilibrium, their mean values grow in absolute value, with the distance from equilibrium. While the dissipation at the cold thermostat contracts the phase space volumes, the hot thermostat expands them. However, ξ_C dissipates more than ξ_H creates, leading, on average, to a positive global dissipation in the steady state.

To test the Transient Fluctuation Relation (3.4), we have numerically computed the probability distribution function of the dissipation function (3.9), for different values of the transient time τ, and for a channel of $L = 10$ cells with $n = 4$ particles per cell. This test may seem unnecessary, because our dynamics is time reversal invariant, which is the only condition required for (3.4) to hold. In reality, there are two subtle points, at least, which make non-trivial the test: a) our simulations are not exactly reversible, because of the numerical scheme approximating the solution of the equations of motion, and because of round-off errors; b) the initial continuous ensemble f, required by the theory, is replaced by a finite number of initial states, supposed to be picked up at random with density f. This, combined with the fact that the dissipation takes place discontinuously in time, because it relies on the interactions between thermostated disks and point particles, makes delicate the choice of the numerical procedure, which could introduce spurious effects, leading to fluctuations that do not satisfy the Transient Fluctuation Relation. Such spurious effects could spoil also the tests of the Steady State Fluctuation Relation which, differently from the Transient Fluctuation Relation, requires more than time reversibility to hold, and certainly needs to be tested case by case.

Therefore, the test of the Transient Fluctuation Relation is rather important, in our system, to calibrate the numerical protocols. Our investigation has shown that the effect of the numerical integration on time reversibility is negligible, as far as (3.4) is concerned, but also that the construction of the initial ensemble needs special care. What proved adequate

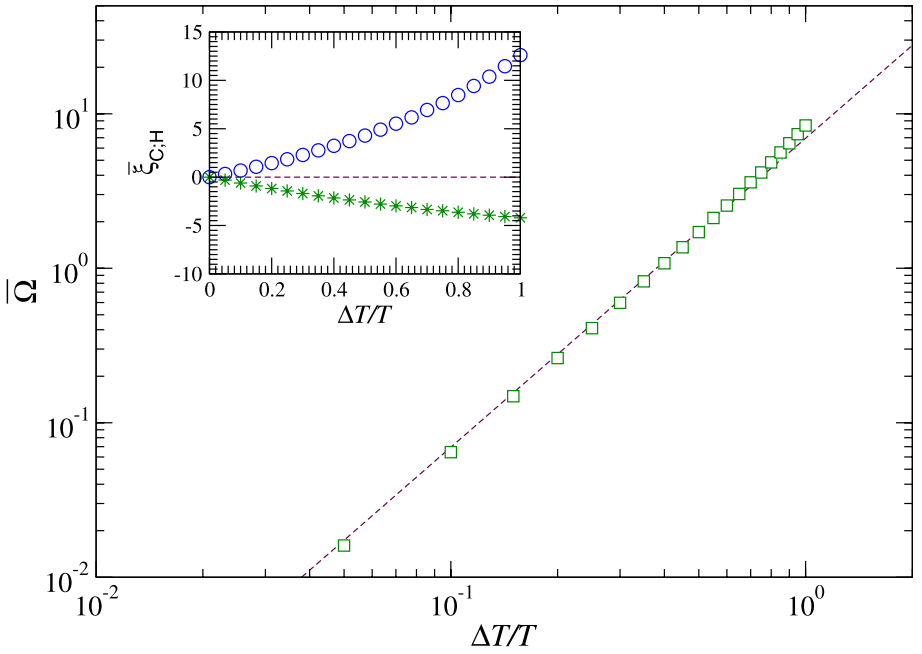

Fig. 6 Long time average in the steady state of the dissipation function $\Omega = \frac{\Delta T}{T}(\xi_C - \xi_H)$ as a function of the relative temperature gradient $\Delta T/T$. The *dashed line* corresponds to $(\Delta T/T)^2$. *Inset*: local phase space contraction rate, $\overline{\xi}_C$ (*circles*), and $\overline{\xi}_H$ (*stars*)

to our purpose is the construction of f from an equilibrium simulation, which generates a collection of decorrelated microstates, by saving a microstate every sufficiently long time.

We have proceed as follows: at $t = 0$ the state of the system is set to a microstate previously generated by the equilibrium dynamics at a temperature $T_0 = (T_C + T_H)/2$. From this initial state, the temperatures of the thermostats are set to T_C and T_H respectively. Then, the system evolved for a certain time τ, and $\overline{\Omega}_{0,\tau}$ was computed. Considering a large ensemble of such processes, the empirical probability distribution function $P(\overline{\Omega}_{0,\tau})$ was constructed.

Furthermore, we define

$$\mathcal{C}_\Omega(\tau; A) \equiv \frac{1}{\tau} \ln \frac{P(\overline{\Omega}_{0,\tau} \in A_\delta^+)}{P(\overline{\Omega}_{0,\tau} \in A_\delta^-)}, \tag{3.10}$$

where A is the centre of the corresponding bin of the empirical distribution. In terms of (3.10), the transient Ω-FR is written as

$$\mathcal{C}_\Omega(\tau; A) = A; \quad \text{for all } \tau. \tag{3.11}$$

We have verified the Transient Fluctuation Relation for several values of $\tau \in [0.01, 20]$, for a temperature gradient given by $T_C = 700$ and $T_H = 1300$. These results are shown in Fig. 7 for the slope of the relation (3.11). In the inset of Fig. 7 we show $P(\overline{\Omega}_{0,\tau})$ for four values of τ. We have found that for small τ, the obtained distribution is highly asymmetric. It becomes Gaussian only for large τ.

The verification of (3.11) indicates that our numerical procedure is appropriate to test the Ω-FRs, hence that it may be used to test the Steady State Fluctuation Relation.

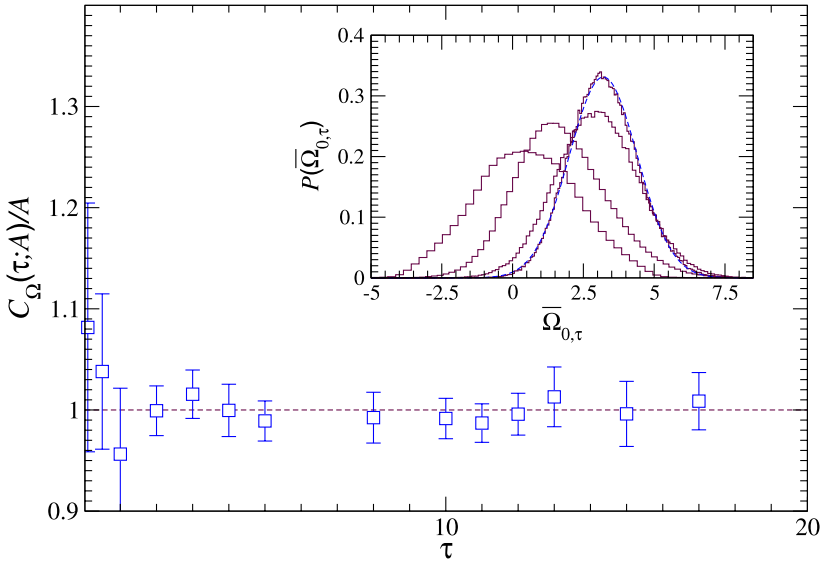

Fig. 7 The slope of $C_\Omega(A,\tau)$ as a function of τ, for a channel of 10 cells, $T_C = 700$ and $T_H = 1300$. *Inset*: Probability distribution function $P(\overline{\Omega}_{0,\tau})$ for (from left to right) $\tau = 1$, 5, 10 and 15. The *dashed line* corresponds to a Gaussian function

3.3 Steady State Fluctuation Relation

The steady state fluctuation relation obtained by Evans, Cohen and Morriss in [2] was motivated by the fact that the phase space contraction rate Λ is proportional to the energy dissipation rate divided by the temperature, for a subclass of Gaussian isoenergetic particle systems, which includes the model of [2]. This way the fluctuation relation for Λ, which we call Λ-FR as in [16], could be given a physical meaning in [2]. The Λ-FR has been later proved by Gallavotti and Cohen to hold for all dissipative, time reversible, smooth and uniformly hyperbolic dynamical systems, independently of their physical meaning [13, 14]. For such systems, the Λ-FR states that:

$$\lim_{\tau\to\infty} \frac{1}{\tau\langle\Lambda\rangle_\infty} \log \frac{P(\hat{\Lambda}_\tau \in A_\delta^+)}{P(\hat{\Lambda}_\tau \in A_\delta^-)} = A, \tag{3.12}$$

where $\hat{\Lambda}_\tau = \overline{\Lambda}_{0,\tau}/\langle\Lambda\rangle_\infty$ is the phase space contraction rate averaged during a time interval τ and normalized to its stationary state value $\langle\Lambda\rangle_\infty$, and $P(\hat{\Lambda})$ is the corresponding steady state probability distribution function. The Λ-FR is supposed to be valid only if $\langle\Lambda\rangle_\infty \neq 0$ and A belongs to a given interval.

In [16], it has been shown that the steady state fluctuation relations may only rely on the time reversibility of the microscopic dynamics and on the time behaviour of the quantity $\mathcal{B}_\Omega$, defined in (3.14) below, independently of the fluctuating odd observable under consideration. This way, Ω appears to be a sort of *"thermodynamic potential"*, which determines the behaviour of all other odd observables, but works even far from equilibrium.[6] This can

[6] In the mathematical theory of smooth, uniformly hyperbolic dynamical systems, it is Λ that plays a role analogue to that of a "thermodynamic potential".

be understood starting from the symmetry relation (3.3), concerning the fluctuations of any observable that is odd with respect to time reversal. In (3.3), the symmetry of the fluctuations is expressed in terms of averages of the dissipation function (3.2), with respect to the initial measure μ of density f. Taking the ensemble average with respect to the measure evolved up to time t, μ_t, of the averages of Ω along trajectory segments of duration τ, which at time $t = 0$ started from the initial state μ, one obtains:

$$\frac{1}{\tau} \ln \frac{\mu_t(\overline{\Omega}_{0,\tau} \in A_\delta^+)}{\mu_t(\overline{\Omega}_{0,\tau} \in A_\delta^-)} = A + \epsilon(\delta, t, A, \tau) - \frac{1}{\tau} \ln \mathcal{B}_\Omega(t, \tau), \tag{3.13}$$

where ϵ is bounded by $0 \leq \epsilon < |\delta|$, and $\mathcal{B}_\Omega(t, \tau)$ is a kind of correlation function given by[7]

$$\mathcal{B}_\Omega(t, \tau) = \langle e^{-\Omega_{0,t}} e^{-\Omega_{t+\tau,2t+\tau}} \rangle_{\overline{\Omega}_{t,t+\tau} \in A_\delta^+}. \tag{3.14}$$

If μ_t tends to a steady state μ_∞ when $t \to \infty$, then (3.13) should change from a statement on the ensemble at time t, to a statement on the statistics generated by a single typical trajectory of the stationary state μ_∞. This requires some assumption, because t tends to infinity before τ does and, in principle, the growth of t could make the conditional average in (3.14) diverge. However, if a finite time scale τ_m characterizes the decay of $\tau^{-1} \ln \mathcal{B}_\Omega$,[8] then (3.13) shows that τ_m is the time scale which must be exceeded for the $t \to \infty$ limit to be practically reached. When this is the case, the transient relations yield the steady state ones, in the long time limits [16].

In some cases, the steady state Λ-FR and Ω-FR coincide, as mentioned above, while in other cases they are clearly different. For instance, in some cases in which Λ represents the heat flow, Ω the dissipated energy, and the particles interaction potentials are singular, the tails of the Λ-FR and Ω-FR may be quite different [16, 17, 23–25].[9] Which systems actually enjoy the decay of $\tau^{-1} \ln \mathcal{B}_\Omega(t, \tau)$ required for (3.12) to hold, or for other steady state relations to be derived from (3.3) is not known. Hence a test is necessary in the systems of physical interest.[10] Therefore, we perform the test on our model.

The mesoscopic time scale τ_m, expresses a physical property of the system, typically the mean free time and thus, does not depend on t or τ. If $t, \tau \gg \tau_m$, the boundary terms $\overline{\Omega}_{t-\tau_m,t}$ and $\overline{\Omega}_{t+\tau,t+\tau+\tau_m}$, are typically small compared to $\overline{\Omega}_{t,t+\tau}$. For this not to be the case, some singularity of Ω must occur within $(t - \tau_m, t)$ or $(t + \tau, t + \tau + \tau_m)$. However, even in that case, similar events may equally likely occur in the intervals $(0, t)$ and $(t + \tau, 2t + \tau)$, hence $\overline{\Omega}_{t-\tau_m,t}$ and $\overline{\Omega}_{t+\tau,t+\tau+\tau_m}$ are expected to contribute only a fraction of order $\mathcal{O}(\tau_m/\tau)$ to the

[7] Although the aspect of $\mathcal{B}_\Omega(t, \tau)$ resembles that of a standard correlation function, it cannot be always interpreted like that. For instance, in cases which verify the modified FR of axiom C systems, which enjoy a strong form of correlations decay [40–43], the term $\tau^{-1} \ln \mathcal{B}_\Omega(t, \tau)$ does not decay, if Ω is chosen to equal Λ. In other cases in which no FR is verified, such as those with trivial steady states considered in [20, 21], $\mathcal{B}_\Omega(t, \tau)$ grows exponentially with t, as simple calculations show. Because the $t \to \infty$ limit must be taken before the $\tau \to \infty$ limit, this illustrates that the transient FR cannot not turn into a steady state FR, in these cases, although the transient FR holds at all times. A more detailed discussion of these facts can be found in [1, 16].

[8] Note that $\mathcal{B}_\Omega$ is computed with respect to the initial measure μ, even for $t > 0$.

[9] This behaviour was first obtained for a stochastic model, namely the Brownian particle dragged in a liquid by a moving harmonic potential [23, 24]. Later, the corresponding extended Λ-FR has been derived for observables for which the probability distribution function has exponential tails [25].

[10] It is known, however, that $\tau^{-1} \ln \mathcal{B}_\Omega$ has to decay in systems not too far from equilibrium, i.e. in the linear regime of Irreversible Thermodynamics, for the transport coefficients to exist [1, 16].

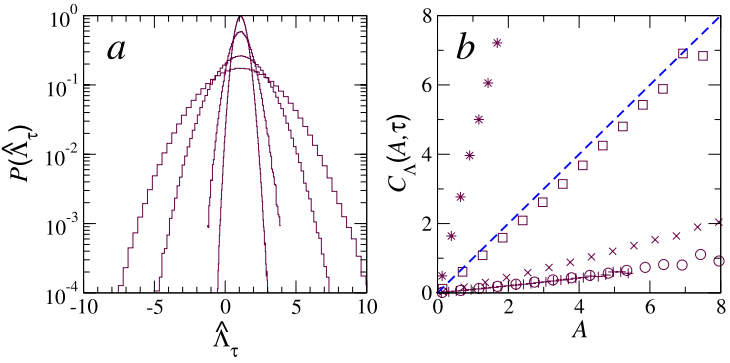

Fig. 8 (**a**) Probability distribution $P(\Lambda_\tau)$ for $\tau = 1$, 10, 20 and 40. The largest the τ the more narrow the distribution gets. The data was obtained for a channel of $L = 10$ cells with a density of $n = 4$ particles per cell. The temperatures of the thermostats were set to $T_C = 700$ and $T_H = 1300$. (**b**) $C_\Lambda(\tau; A)$ as a function of A for different values of τ: 0.1 (*stars*), 0.5 (*squares*), 1 (*crosses*), 5 (*circles*) and 10 (*pluses*). The *dashed line* corresponds to the line with slope 1. As observed, $C_\Lambda(\tau; A)$ is approximately linear with A, for all τ, with a slope $\neq 1$, that depends on τ (see Fig. 9 below). Note that $P(\Lambda_\tau)$ are not symmetric about their maximum. Therefore, for the values of τ considered, $P(\Lambda_\tau)$ is not Gaussian, but their tails decay as fast as Gaussian

arguments of the exponentials in (3.14). Therefore, in the cases of thermodynamic interest, one can write

$$\begin{aligned}\mathcal{B}_\Omega(t,\tau) &\approx \left\langle e^{-\Omega_{0,t-\tau_m}} \cdot e^{-\Omega_{t+\tau+\tau_m,2t+\tau}} \right\rangle_{\overline{\Omega}_{t,t+\tau}\in A_\delta^+} \\ &\approx \left\langle e^{-\Omega_{0,t-\tau_m}} \cdot e^{-\Omega_{t+\tau+\tau_m,2t+\tau}} \right\rangle \\ &\approx \left\langle e^{-\Omega_{0,t+\tau_m}} \right\rangle \left\langle e^{-\Omega_{t+\tau+\tau_m,2t+\tau}} \right\rangle \\ &\approx \mathcal{O}(1), \end{aligned} \tag{3.15}$$

with an accuracy which improves when t and τ are growing multiples of the time τ_m. The last line is just a statement of the conservation of probability and of the fact that $\mathcal{B}_\Omega$ typically decays within microscopic times [1]. One then realizes that $\mathcal{B}_\Omega(t,\tau)$ tends to approximately 1 as $1/\tau$, with a characteristic scale of order $\mathcal{O}(\tau_m)$, which leads to the validity of the steady state Ω-FR. Then, for sufficiently small δ, and large t and τ the relation

$$\frac{1}{\tau} \ln \frac{\mu_t(\overline{\Omega}_{t,t+\tau} \in A_\delta^+)}{\mu_t(\overline{\Omega}_{t,t+\tau} \in A_\delta^-)} \approx A \tag{3.16}$$

holds, and remains valid in the $t \to \infty$ limit. If P is the corresponding steady state probability distribution function, one can rewrite (3.16) as

$$\mathcal{C}_{\Omega_\infty}(\tau; A) \equiv \frac{1}{\tau} \ln \frac{P(\overline{\Omega}_{0,\tau} \in A_\delta^+)}{P(\overline{\Omega}_{0,\tau} \in A_\delta^-)} \approx A; \quad \text{for } \tau > \tau_m, \tag{3.17}$$

which we call steady state Ω-FR.

We have measured the steady state fluctuations of Λ and of Ω, for the model introduced in Sect. 2. Let us first describe those of Λ, and then compare them with those of Ω, in the $\tau \to \infty$ limit.

We consider a channel of length $L = 10$ cells and $n = 4$ particles per cell. As before, the disks in the leftmost and rightmost cells are coupled to Nosé-Hoover thermostats with $T_C = 700$ and $T_H = 1300$ respectively, and $\tau_{th} = 1$. Starting from a random initial state we leave the system relax for a time corresponding to 5×10^6 collisions of the particles with the disks. This relaxation time ensures that the system has reached its stationary state at which, the mean heat current is uniform. Using (2.7), in the stationary state we measure the values of the phase space contraction rate Λ each 10^{-3} time units. We then compute the time average $\overline{\Lambda}_{0,\tau}$, from disconnected intervals of the time series of Λ. Finally, we compute the empirical probability distribution function of $\overline{\Lambda}_{0,\tau}$, normalized to its steady state value $\langle\Lambda\rangle_\infty$.

We have found that, for our system, the unboundness of Λ is not associated with exponential tails in its probability distribution. This is shown in Fig. 8a, where $P(\hat{\Lambda}_\tau)$ is plotted for different values of τ: within numerical accuracy, $P(\hat{\Lambda}_\tau)$ has Gaussian tails for all values of τ. Note, however, that for the values of τ considered, $P(\hat{\Lambda}_\tau)$ is not Gaussian.

To discuss the behaviour of the Λ-FR (3.12) for finite averaging times τ, we define, as before,

$$\mathcal{C}_\Lambda(\tau; A) \equiv \frac{1}{\tau\langle\Lambda\rangle_\infty} \ln \frac{P(\hat{\Lambda}_\tau \in A^+_\delta)}{P(\hat{\Lambda}_\tau \in A^-_\delta)}, \tag{3.18}$$

so that the relation (3.12)), for finite but sufficiently large τ, would imply that $\mathcal{C}_\Lambda(\tau; A)/A \approx 1$. In panel b of Fig. 8, the dependence of $\mathcal{C}_\Lambda(\tau; A)$ on A is shown for different values of τ. Independently of the value of τ, $\mathcal{C}_\Lambda(\tau; A)$ is approximately linear in A. The only dependence on τ is the slope of $\mathcal{C}_\Lambda(\tau; A)$ and the value of A at which the statistical errors become large. This is different from recent findings for other Nosé-Hoover thermostated systems. In [26] the Nosé-Hoover thermostated Lorentz gas was studied, and it was found that the fluctuations of Λ obeying the Λ-FR are only those that are smaller in magnitude than the steady state mean $\langle\Lambda\rangle_\infty$. Larger heat fluctuations follow the extended version of the Λ-FR of [23–25], which saturates at some value. In these works, the deviation from the standard Λ-FR was supposed to be due to the singularities of Λ, which may produce exponential tails in the probability distribution function of Λ, possibly as a consequence of the exponential tails of the distribution function of the values of H.

Our results confirm that the identification of deterministic particle systems which verify a modified version of the FR is far from obvious [16, 17]. Indeed, the most common situation which is found in the specialized literature, as well as here, is that even systems with singular Λ verify the standard FR, since the tails of the distribution of the fluctuations of Λ decay as fast as Gaussian tails. Then, as explained e.g. in Ref. [25], the standard FR must hold. In our case, the phase space contraction rate Λ is unbounded because of the logarithmic potential present in the Nosé Hamiltonian (2.3), but the tails of the distributions of its fluctuations appear to be Gaussian, and $\mathcal{C}_\Lambda(\tau; A)$ turns out to be linear in A, even for fluctuations much larger than $\langle\Lambda\rangle_\infty$.

We now discuss the behaviour of $\mathcal{C}_\Lambda(\tau; A)$ with τ. In Fig. 9, the slope of the $\mathcal{C}_\Lambda(\tau; A)$ (squares), is shown as a function of τ. These values were obtained from a best fit to a linear function of $\mathcal{C}_\Lambda(\tau; A)$. For small times τ, shorter than the mesoscopic time scale τ_m, the slope of $\mathcal{C}_\Lambda(\tau; A)$ decreases approximately as $\sim 1/\tau$. The slope reaches a minimum value, after which $\mathcal{C}_\Lambda(\tau; A)/A$ increases, seemingly converging to its asymptotic value 1. This convergence becomes clearer in the inset of Fig. 9, where the same data has been plotted as a function of $1/\tau$. These results are consistent with an exponential convergence of $\mathcal{C}_\Lambda(\tau; A)/A$ to 1 as $\tau \to \infty$ (the dashed line in the inset of Fig. 9, corresponds to an

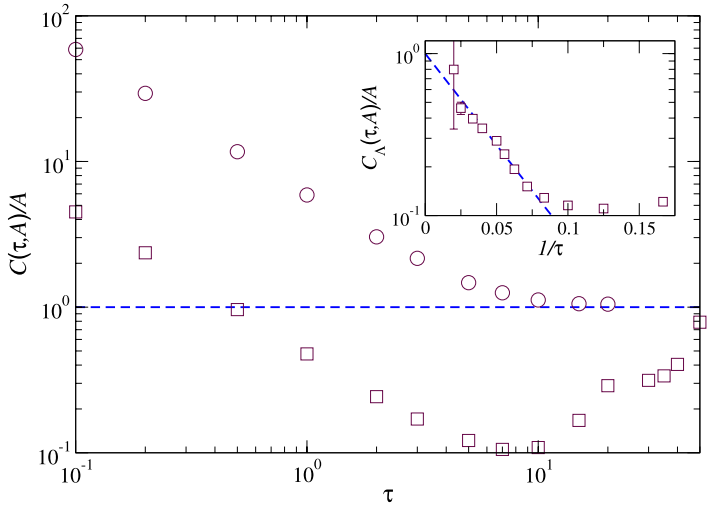

Fig. 9 Comparison between the slopes of $\mathcal{C}_\Lambda(\tau; A)$ (*squares*), and $\mathcal{C}_{\Omega_\infty}(\tau; A)$ (*circles*), as a function of the averaging time τ. The parameters are as indicated in Fig. 8. In the *inset*, $\mathcal{C}_\Lambda(\tau; A)/A$ is plotted in inverse units of τ. The *dashed line* corresponds to the function $e^{-26/\tau}$

exponential scaling of $\exp(-26/\tau)$). Recalling (3.8), and the fast convergence of the Ω-FR, one may think that the monotonic convergence of the Λ-FR goes as $1/\tau$, rather than exponentially. Indeed, in the cases in which Λ is bounded, a conservative estimate of the convergence rate yields $(\Lambda_M - \Lambda_m)/\tau$, where Λ_M and Λ_m are the maximum and minimum values of Λ, see e.g. [17]. However, convergence may be faster even when Λ has no bounds, as in our case. Therefore, the steady state fluctuations of the phase space contraction rate for our model system satisfy the Λ-FR (3.12).

Let us now turn to the steady state Ω-FR (3.17) and compare its behaviour at large averaging times τ with that of the fluctuations of the Λ-FR. Figure 9 shows the slope of $\mathcal{C}_{\Omega_\infty}(\tau; A)$ (circles), as a function of τ. For times shorter than the mesoscopic time scale τ_m, the steady state fluctuation relations of Λ and of Ω converge with an error which decays as $1/\tau$. At longer times ($\tau > \tau_m$) the slope of $\mathcal{C}_{\Omega_\infty}$ is fixed to 1, indicating that the steady state Ω-FR (3.16) holds. Moreover, Fig. 9 shows that the convergence of $\mathcal{C}_{\Omega_\infty}$ is much faster than that of $\mathcal{C}_\Lambda$, as expected because of the total derivative by which Ω and Λ differ. Indeed, we observed that the turning point of the convergence of the Λ-FR occurs when $\mathcal{B}_\Omega$ has decayed, and the Ω-FR has converged, i.e. when only the term in H is left to decay. The difference in convergence rates is expected to grow when the system approaches equilibrium, and the dissipative part of Λ becomes dominated by the total derivative $\dot{H}$.[11]

These observations support the idea of [16] that the scale set by the decay of $\tau^{-1} \ln \mathcal{B}_\Omega$ determines the behaviour of the fluctuations of all odd observables, in our model, although the global behaviour of different observables may be different. To test this we have computed the behaviour of $\mathcal{B}_\Omega(t, \tau)$. We considered a chain of $L = 10$ cells, density $n = 4$ particles per cell and $T_C = 700$, $T_H = 1300$. As in Sect. 3.2, at $t = 0$ the system is set to an equilibrium

[11] Similar observations were made in [18], where the issue of convergence rates of FRs was thoroughly investigated in models of shearing fluids. In the case of [18], the convergence of the Λ-FR appeared so much slower than that of the Ω-FR, that it could not be directly observed, and was only indirectly inferred.

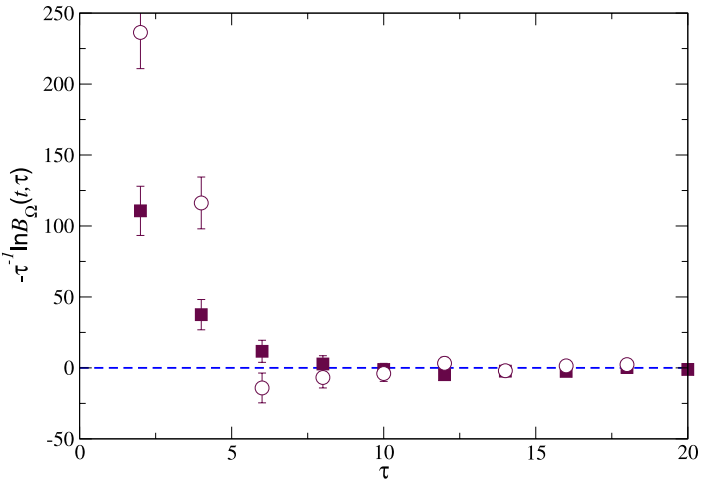

Fig. 10 Logarithm of $\mathcal{B}_\Omega(t,\tau)$ of (3.14) as a function of the averaging time τ, for $t=1$ (*solid squares*) and $t=10$ (*open circles*), for $A=2$ and $\delta=0.1$. The rest of the parameters are as indicated in Fig. 8

microstate at temperature $T_0=(T_C+T_H)/2$. With the temperature of the thermostats set to T_C and T_H respectively, we follow the evolution of the system for a time $2t+\tau$ and compute the time averages of $\Omega_{0,t}$, $\Omega_{t,t+\tau}$ and $\Omega_{t+\tau,2t+\tau}$. Finally, using (3.14) and a large ensemble of such processes, we obtain $\mathcal{B}_\Omega(t,\tau)$. Figure 10 shows the dependence of $-\tau^{-1}\ln\mathcal{B}_\Omega(t,\tau)$ on τ for $A=2$, $\delta=0.1$, and $t=1$ (solid squares) and $t=10$ (open circles). For both values of t, $-\tau^{-1}\ln\mathcal{B}_\Omega(t,\tau)$ decays, and reaches zero within numerical accuracy, for times $\tau_m\approx 10$. This time scale coincides approximately with the time scale at which, $\mathcal{C}_{\Omega_\infty}/A$ converges to its asymptotic value 1, and $\mathcal{C}_\Lambda/A$ starts its monotonic convergence.

4 Conclusions

We have discussed the behaviour of the transient and steady state fluctuations of the phase space contraction rate and of the dissipation function, in a Nosé-Hoover thermostated system. The dynamics in the bulk of the system is purely Hamiltonian, hence preserves the phase space volumes. Two Nosé-Hoover thermostats, are coupled to *d.o.f.* that are fixed at the boundaries of the system.

We have studied the dynamics of the local thermostats and have characterized the equilibrium and nonequilibrium states of the system. In the equilibrium state, we have shown that the effective interaction among the particles is sufficient to ergodize the, otherwise regular, dynamics of the thermostat. This leads to a local thermalization of all the *d.o.f.* of the system, for $\Delta T/T<1$ (which is our case). Out of equilibrium, when the temperatures of the thermostats are unequal, the system develops nonequilibrium temperature and density profiles. Consequently, a stationary and uniform heat current appears, transporting heat from the hot to the cold reservoir. Energy is then dissipated at a constant rate, measured by the dissipation function.

We have found that the transient fluctuations of Ω do satisfy the transient Ω-FR, indicating that our numerical solution of the equations of motion and generation of the equilibrium ensemble from the equilibrium dynamics are appropriate.

For the system studied in this paper, in which Λ does not coincide with the energy dissipation rate Ω, the fluctuations of both quantities obey the same symmetry given by the standard steady state FR, in the $\tau \to \infty$ limit. In particular, the standard Λ-FR is verified despite the fact that Λ is unbounded, because the tails of the distribution of its fluctuations decay as fast as Gaussian tails. The Λ-FR needs $\tau^{-1} \ln \mathcal{B}_\Omega$ to have decayed, before starting a monotonic convergence, while the Ω-FR appears to have converged, within numerical accuracy, after those times. This different behaviour depends on the total derivative $\dot{H}$, which distinguishes Λ from Ω. The characteristic time scale of the decay of $\tau^{-1} \ln \mathcal{B}_\Omega$ is the mesoscopic time scale τ_m.

Acknowledgements The authors are indebted to D.J. Evans, for enlightening discussions and invaluable correspondence. We thank the anonymous referees for their very detailed and enlightening remarks that lead to a substantial improvement of the paper. We thank Fondazione CRT for financial support.

References

1. Rondoni, L., Mejia-Monasterio, C.: Nonlinearity **20**, R1 (2007)
2. Evans, D.J., Cohen, E.G.D., Morriss, G.P.: Phys. Rev. Lett. **71**, 2401 (1993)
3. Parry, W.: Commun. Math. Phys. **106**, 267 (1986)
4. Vance, W.N.: Phys. Rev. Lett. **69**, 1356 (1992)
5. Evans, D.J., Searles, D.J.: Adv. Phys. **52**, 1529 (2002)
6. Evans, D.J., Searles, D.J.: Phys. Rev. E **52**, 5839 (1995)
7. Evans, D.J., Searles, D.J.: Phys. Rev. E **50**, 1645 (1994)
8. Searles, D.J., Ayton, G., Evans, D.J.: AIP Conf. Ser. **519**, 271 (2000)
9. Evans, D.J., Searles, D.J.: J. Chem. Phys. **113**, 3503 (2000)
10. Williams, S.R., Searles, D.J., Evans, D.J.: Phys. Rev. E **70**, 066113 (2004)
11. Williams, S.R., Searles, D.J., Evans, D.J.: J. Chem. Phys. **124**, 194102 (2006)
12. Wang, G.M., Sevick, E.M., Mittag, E., Searles, D.J., Evans, D.J.: Phys. Rev. Lett. **89**, 050601 (2002)
13. Gallavotti, G., Cohen, E.G.D.: Phys. Rev. Lett. **94**, 2694 (1995)
14. Gallavotti, G., Cohen, E.G.D.: J. Stat. Phys. **80**, 931 (1995)
15. Gallavotti, G.: Math. Phys. Electronic J. **1**, 1 (1995)
16. Searles, D.J., Rondoni, L., Evans, D.J.: J. Stat. Phys. **128**, 1337 (2007)
17. Evans, D.J., Searles, D.J., Rondoni, L.: Phys. Rev. E **71**, 056120 (2005)
18. Zamponi, F., Ruocco, G., Angelani, L.: J. Stat. Phys. **115**, 1655 (2004)
19. Zamponi, F.: J. Stat. Mech. P02008 (2007)
20. Cohen, E.G.D., Gallavotti, G.: J. Stat. Phys. **96**, 1343 (1999)
21. Lepri, S., Rondoni, L., Benettin, G.: J. Stat. Phys. **99**, 857 (2000)
22. Posch, H.A., Hoover, W.G.: Physica D **187**, 281 (2004)
23. van Zon, R., Cohen, E.G.D.: Phys. Rev. Lett. **91**, 110601 (2003)
24. van Zon, R., Cohen, E.G.D.: Phys. Rev. E **69**, 056121 (2004)
25. Bonetto, F., Gallavotti, G., Giuliani, A., Zamponi, F.: J. Stat. Phys. **123**, 39 (2006)
26. Gilbert, T.: Phys. Rev. E **73**, 035102 (2006)
27. Mejia-Monasterio, C., Larralde, H., Leyvraz, F.: Phys. Rev. Lett. **86**, 5417 (2001)
28. Larralde, H., Leyvraz, F., Mejia-Monasterio, C.: J. Stat. Phys. **113**, 197 (2003)
29. Eckmann, J.-P., Young, L.-S.: Commun. Math. Phys. **262**, 237 (2006)
30. Eckmann, J.-P., Mejia-Monasterio, C., Zabey, E.: J. Stat. Phys. **123**, 1339 (2006)
31. Hoover, W.G.: Phys Rev. A **31**, 1695 (1985)
32. Nosé, S.: J. Chem. Phys **81**, 511 (1984)
33. Evans, D.J., Morris, G.P.: Statistical Mechanics of Nonequilibrium Liquids. Academic Press, New York (1990)
34. Rateitschak, K., Klages, R., Hoover, Wm.G.: J. Stat. Phys. **101**, 61 (2000)
35. Hoover, W.G., Aoki, K., Hoover, C.G., De Groot, S.V.: Physica D **187**, 253 (2004)
36. Dhar, A., Dhar, D.: Phys. Rev. Lett. **82**, 480 (1999)
37. Evans, D.J., Searles, D.J.: Adv. Phys. **51**, 1529 (2002)
38. Searles, D.J., Evans, D.J.: Int. J. Thermophys. **22**, 123 (2001)
39. Gallavotti, G.: Ann. Inst. Poincarè **70**, 429 (1999)
40. Bonetto, F., Gallavotti, G.: Commun. Math. Phys. **189**, 263 (1997)
41. Bonetto, F., Gallavotti, G., Garrido, P.L.: Physica D **105**, 226 (1997)
42. Rondoni, L., Morriss, G.P.: Open Syst. Inf. Dynam. **10**, 105 (2003)
43. Gallavotti, G., Rondoni, L., Segre, E.: Physica D **187**, 338 (2004)